ASTM INTERNATIONAL

Geotechnical Testing Journal

Bruna G. O. Ribeiro,[1] Minyong Lee,[1] and Michael G. Gomez[2]

DOI: 10.1520/GTJ20230302

An Examination of the Effect of Chemically Induced Damage on the Monotonic and Cyclic Shearing Behavior of Biocemented Sands

Copyright by ASTM Int'l (all rights reserved) Tue Jul 18 19:37:22 GMT 2023
Downloaded/printed by
University of Washington pursuant to License Agreement. No further reproductions authorized.

Geotechnical Testing Journal

doi:10.1520/GTJ20230302 available online at www.astm.org

Bruna G. O. Ribeiro,[1] Minyong Lee,[1] and Michael G. Gomez[2]

An Examination of the Effect of Chemically Induced Damage on the Monotonic and Cyclic Shearing Behavior of Biocemented Sands

Reference

B. G. O. Ribeiro, M. Lee, and M. G. Gomez, "An Examination of the Effect of Chemically Induced Damage on the Monotonic and Cyclic Shearing Behavior of Biocemented Sands," *Geotechnical Testing Journal* https://doi.org/10.1520/GTJ20230302

ABSTRACT

Microbially induced calcite precipitation is a biomediated soil improvement method that can improve the engineering properties of granular soils. Although improvements in soil engineering behaviors afforded by biocementation have been extensively characterized, there remains limited understanding of the anticipated long-term engineering behavior of biocemented soils following progressive chemical damage that may be experienced following initial applications. In this study, 10 direct simple shear tests were performed to investigate the effect of chemically induced damage on the drained monotonic and undrained cyclic shearing behaviors of biocemented loose Ottawa F-65 sand. All specimens were either uncemented, biocemented to different cementation levels corresponding to shear wave velocity increases (ΔV_s) between 150 and 500 m/s, or biocemented to a ΔV_s near 250 or 500 m/s and then subjected to degradation injections, which induced chemical damage and achieved ΔV_s reductions of either 100 or 200 m/s. For all specimens, V_s and soil calcium carbonate content measurements were performed to assess improvement magnitudes, cementation uniformity, and evaluate magnitudes of chemically induced damage. As expected, increases in biocementation levels as captured by V_s increases were shown to progressively improve drained monotonic and undrained cyclic shearing behaviors. Following chemically induced damage, however, behavioral improvements were largely retained and were found to be consistent with the nondegraded biocemented specimens on the basis of similar V_s values. The performed tests provide the first examination of the expected long-term engineering behaviors of biocemented sands and yield new understandings regarding the anticipated impacts of chemical damage on behaviors relevant to subsurface liquefaction mitigation applications and other geotechnical use cases.

Manuscript received January 11, 2023; accepted for publication June 12, 2023; published online July 19, 2023.

[1] Department of Civil and Environmental Engineering, University of Washington, More Hall, Room 132G, Seattle, WA 98195, USA, https://orcid.org/0000-0003-3501-9089 (B.G.O.R.), https://orcid.org/0000-0002-7436-5374 (M.L.)

[2] Department of Civil and Environmental Engineering, University of Washington, More Hall, Room 132G, Seattle, WA 98195, USA (Corresponding author), e-mail: mggomez@uw.edu, https://orcid.org/0000-0002-4464-5447

Copyright © 2023 by ASTM International, 100 Barr Harbor Drive, PO Box C700, West Conshohocken, PA 19428-2959

ASTM International is not responsible, as a body, for the statements and opinions expressed in this paper. ASTM International does not endorse any products represented in this paper.

Copyright by ASTM Int'l (all rights reserved) Tue Jul 18 19:37:22 GMT 2023
Downloaded/printed by
University of Washington pursuant to License Agreement. No further reproductions authorized.

Keywords

biocementation, microbially induced calcite precipitation, biomediated, soil improvement, liquefaction, direct simple shear test, biogeotechnics

Introduction

Microbially induced calcite precipitation is a biomediated cementation process that can improve the engineering properties of granular soils through the precipitation of calcium carbonate ($CaCO_3$) minerals on soil particle surfaces and contacts. The resulting biocementation can increase the shear stiffness and shear strength of soils while decreasing soil hydraulic conductivity and porosity (DeJong et al. 2022; Montoya and DeJong 2015; Gomez and DeJong 2017). Biocementation can be performed by injecting water-based solutions containing soluble reactants (e.g., urea and calcium salts) into soils targeted for improvement, with microbial urea hydrolysis allowing for the generation of aqueous carbonate over time and the initiation of $CaCO_3$ precipitation. The process has numerous potential engineering applications including liquefaction mitigation, soil erosion prevention, divalent contaminant immobilization, and improvement of slope stability and foundation capacities (Martinez and DeJong 2009; Jiang and Soga 2019, Xiao et al. 2019; Terzis et al. 2020). Advances in treatment application techniques (Gomez et al. 2018; San Pablo et al. 2020), characterization of the engineering behaviors of biocemented soils (Montoya and DeJong 2015; Zamani et al. 2021; Lee et al. 2022; Cardoso, Vieira, and Borges 2023), and demonstration of the technology at meter-scale (van Paassen et al. 2011; Gomez et al. 2015, 2017; Ghasemi and Montoya 2022) have allowed the technology to progress toward field-scale practical adoption; however, limited understanding of the permanence and performance of biocemented soils has remained a significant knowledge gap. Although past studies have examined the effects of extreme chemical damage events, such as exposure to synthetic acid rain, on the engineering properties of biocemented soils (Chen and Achal 2020; Cheng et al. 2017), there remains limited understanding of the expected mechanical behaviors of biocemented soils subjected to progressive chemical damage, which may occur at field sites over time following initial ground improvement applications.

More recent studies have aimed to improve our understanding of the mineralogy and dissolution behavior of biocementation in an effort to better understand its chemical and mechanical resistance and the implications of subsurface geochemical conditions during and after biocementation applications. For example, Burdalski et al. (2022) investigated the effect of differences in field-representative soil minerals and seawater ions on the morphology and mineralogy of ureolytic biocementation and found that calcite remained the predominant mineral polymorph in all precipitates despite some significant mineralogical and morphological differences. Ribeiro and Gomez (2023) investigated the dissolution behavior of biocemented sands subjected to undersaturated acidic solutions and found that existing dissolution kinetic models could be used to successfully capture the spatial and temporal progression of biocementation chemical damage. Collectively, these studies have improved our understanding of the mineralogical composition and dissolution behaviors of biocemented sands; however, to date, the mechanical behavior of biocemented soils following chemically induced damage has remained unexplored. An improved understanding of the effect of chemical damage on the shearing behavior of biocemented sands over cementation levels ($\Delta V_s = 0$ to 500 m/s) practically relevant to geotechnical applications (DeJong et al. 2022) will be critical for evaluating the resilience and longevity of biocementation soil improvement, beneficial use cases for the technology, and the metrics by which cementation integrity can be effectively characterized in the field following initial improvement.

In this study, a series of direct simple shear (DSS) tests were performed to investigate the shearing behavior of biocemented sands that were either nondegraded or degraded via chemically induced damage. A novel microbially induced fermentation process was employed in these experiments to induce chemical damage and permitted the preparation of chemically degraded biocemented specimens with uniform material properties needed for element-scale testing. Drained monotonic DSS tests investigated the shearing response of nondegraded biocemented sands treated to three different cementation levels ($\Delta V_s = 137$ to 485 m/s), two chemically degraded

Copyright by ASTM Int'l (all rights reserved) Tue Jul 18 19:37:22 EDT 2023
Downloaded/printed by
University of Washington pursuant to License Agreement. No further reproductions authorized.

biocemented specimens that were first cemented to a higher cementation level ($\Delta V_s = 227$ to 480 m/s) and then subsequently degraded to achieve a lower level of improvement ($\Delta V_s = 120$ to 283 m/s), and two uncemented specimens prepared to varying relative densities intended to control for the reduction in void ratio experienced by cemented specimens as the result of added solids from $CaCO_3$ precipitation. Following all monotonic tests, three undrained cyclic DSS tests were performed to investigate the liquefaction triggering and post-triggering behaviors of two nondegraded biocemented sand specimens ($\Delta V_s = 156$ to 247 m/s) as well as the response of a single specimen cemented to a high cementation level ($\Delta V_s = 260$ m/s) and then subsequently degraded to achieve a lower level of improvement ($\Delta V_s = 168$ m/s). Following all tests, observed shearing behaviors were compared between uncemented, nondegraded biocemented, and degraded biocemented specimens and the ability of soil $CaCO_3$ contents and V_s measurements to effectively characterize shearing behaviors before and after chemical damage was investigated. To the best of our knowledge, results from this study provide the first examination of the long-term engineering performance of biocemented sands and yield new insights regarding the chemical resilience of biocementation soil improvement relevant to liquefaction mitigation applications and other geotechnical use cases.

Materials and Methods

SOIL MATERIAL

Ottawa F-65 sand (US Silica, Ottawa, IL), a poorly graded sand (SP) following ASTM D2487-17, *Standard Practice for Classification of Soils for Engineering Purposes (Unified Soil Classification System)*, was used for all tests following previous investigations by Ziotopoulou et al. (2018), Darby et al. (2019), Lee et al. (2022), and others. Ottawa F-65 sand has a D_{50} of 0.21 mm, a coefficient of uniformity of 1.77, a coefficient of curvature of 1.08, and no fines. The sand has a minimum void ratio of 0.51 and a maximum void ratio of 0.78 (Carey, Stone, and Kutter 2020).

DSS APPARATUS

All monotonic and cyclic tests were performed using a cyclic simple shear apparatus (Electromechanical dynamic cyclic simple shear device [EMDCSS], GDS Instruments, Hook, UK), which measured applied axial forces (5 kN range, 0.045 % precision), shear forces (5 kN range, 0.045 % precision), axial displacements (25 mm range, 0.1 % precision), and shear displacements (15 mm range, 0.1 % precision) during all tests. Pinned porous discs (2 mm pin lengths) were used for all specimens in order to mitigate the potential for shear localization at the top platen and soil interface.

SPECIMEN PREPARATION

All biocemented samples were prepared using dry pluviation to a loose initial relative density (D_r) near 35 % and had a diameter of 70.2 mm and a height near 22 mm. After pluviation, specimens were subjected to an initial vertical total stress of 25 kPa. A series of small-strain drained cycles were then applied to precondition samples to promote proper engagement of the specimens at the porous disc and soil interface and establish K_o conditions. During preconditioning, 150 drained cycles with an amplitude of 0.01 mm (0.05 % shear strain) were applied following protocols developed by Humire et al. (2022). After preconditioning, the vertical total stress was increased to 100 kPa and specimens were saturated with deaired deionized water. For uncemented specimens, shearing events were performed immediately after saturation; however, for all biocemented specimens, augmentation and cementation treatments were initiated after saturation. Specimen void ratios were determined for conditions immediately prior to shearing events by collecting and oven-drying sand specimens after testing, measuring total dry masses, accounting for added $CaCO_3$ masses for all biocemented samples using $CaCO_3$ content measurements, and using the densities of $CaCO_3$ and quartz to determine increases in solid volumes resulting from biocementation. Pore volumes for all specimens varied between 32 and 35 mL.

Copyright by ASTM Int'l (all rights reserved) Tue Jul 18 19:37:22 EDT 2023
Downloaded/printed by
University of Washington pursuant to License Agreement. No further reproductions authorized.

SHEAR WAVE VELOCITY MEASUREMENTS

Shear wave velocity (V_s) measurements were completed using bender-extender elements (Lings and Greening 2001) that were fixed at the center of DSS specimen top and bottom end platens. The relative position of bender element sensors was controlled and aligned using horizontal linear variable differential transformer measurements and remained fixed following initial specimen preparation during both cementation and degradation injections until shearing was initiated. Bender elements were excited using a 24 V, 100 Hz square wave, and received signals were measured and recorded using a digital oscilloscope. V_s values were determined from sensor spacings and shear wave transmission and arrival times. For uncemented specimens, V_s measurements were performed before all shearing events. For all nondegraded and degraded biocemented specimens, V_s measurements were performed (1) before and immediately after augmentation, (2) before, immediately after, and 24 h after cementation injections, (3) before, immediately after, 24 h after, and 48 h after degradation injections (when applicable), and (4) immediately before shearing events. Following undrained cyclic shearing, all specimens were slowly recentered back to their initial position while maintaining the vertical stress after failure (≈0 kPa), specimens were then reconsolidated back to the initial vertical stress of 100 kPa, and final V_s measurements were performed at the same horizontal position as all other measurements while accounting for specimen height differences.

CEMENTATION INJECTIONS

Both nondegraded and degraded biocemented specimens were augmented with *Sporosarcina pasteurii* (*S. pasteurii*; American Type Culture Collection [ATCC] 11859) cells that were injected into specimens after saturation in order to achieve sufficient ureolytic activity needed to enable the biocementation process. *S. pasteurii* cells were cultured in sterile ATCC 11859 growth media (0.13 M tris base, 20 g/L yeast extract, 10 g/L ammonium sulfate, pH-adjusted to 9.0), which was inoculated with a frozen stock *S. pasteurii* culture. Inoculated growth media was incubated for 48 h at 30°C using a double-orbital shaker at a shaking speed of 150 r/min. Following incubation, *S. pasteurii* cells were pelleted and rinsed using isotonic saline (9 g/L sodium chloride), and a microplate spectrophotometer was used to measure the optical density of *S. pasteurii* cell pellets at a wavelength of 600 nm (OD_{600}). Measured OD_{600} values for cell pellets corresponded to total cell densities near 2×10^9 cells/mL, and cell pellets were diluted in augmentation solutions that contained 10 mM urea, 100 mM ammonium chloride (NH_4Cl), and 0.2 g/L yeast extract in deionized water to achieve cell densities near 5×10^7 cells/mL. DSS specimens were augmented using 250 mL augmentation solution volumes following injection procedures similar to those by Lee et al. (2022), which involved applying 4 alternating 75 mL injections from bottom to top and top to bottom, intended to achieve uniform cell distributions prior to cementation. After injections, augmentation solutions remained within specimens for at least 1 h to promote cell attachment to soil surfaces.

Following augmentation, 150 mL cementation solution injections were applied to all nondegraded and degraded biocemented specimens once daily for between 1 and 3 days to initiate biocementation improvement. Cementation solutions contained 100 mM NH_4Cl and equimolar urea and calcium chloride ($CaCl_2$) concentrations of either 300 or 700 mM. The presence of soluble calcium in cementation injections allowed for $CaCO_3$ precipitation to occur using *S. pasteurii* cells established in the earlier augmentation injections. Solution urea and $CaCl_2$ concentration magnitudes and cementation injection numbers were varied to achieve different levels of improvement as determined by V_s measurements. Following all cementation injections, specimens were resaturated with deionized deaired water to remove reacted solutions and achieve full saturation. Axial and horizontal displacement measurements during all injections indicated that treatments had no significant effects on specimens and that the initial stress state present following initial preparation was maintained during both augmentation and cementation injections.

DEGRADATION INJECTIONS

Three degraded biocemented specimens were subjected to degradation injections to examine the mechanical behavior of biocemented sands following chemically induced damage. Prior to degradation injections, the

Copyright by ASTM Int'l (all rights reserved) Tue Jul 18 19:37:22 EDT 2023
Downloaded/printed by
University of Washington pursuant to License Agreement. No further reproductions authorized.

degraded biocemented specimens were resaturated with deionized deaired water to remove reacted solutions following biocementation. Following rinsing with deionized deaired water, 150 mL degradation injections were applied to specimens once every 48 h to induce uniform dissolution within specimens using a microbial fermentation process. Degradation solutions were not acidic but rather contained 25 g/L glucose (a fermentable carbohydrate) and 5 g/L yeast extract (a nutrient source needed for fermentative cell growth) and were inoculated with a fermentative bacterial culture obtained from enrichment of a natural sand with a similar solution. The degradation process allowed for inert chemical species (e.g., glucose and yeast extract) to be applied to DSS specimens without inducing chemical degradation. However, upon establishing sufficient fermentation microbial activity, the supplied glucose was fermented over the injection rest periods, thereby producing complex mixtures of organic acids, which permitted the dissolution of previously established cementation. Although microbial fermentation is ubiquitous in the environment, the employed treatment processed was similar to other recent studies examining the use of microbial fermentation to control colloidal silica grouts (Muchongwe 2021) and afforded degradation of cementation in a spatially uniform manner that could not have been achieved using abiotic acid-based injections (Ribeiro and Gomez 2023). During degradation injections, V_s values were monitored and injections proceeded until targeted levels of cementation degradation ($\Delta V_s \approx 100$ and 200 m/s reduction) were achieved. After degrading specimens to the intended final V_s values, degradation injections were terminated, specimens were again resaturated with deaired deionized water, and shearing events were initiated after saturation. The initial stress states established following initial preparation and present during both augmentation and cementation injections were also maintained during all degradation injections.

DRAINED MONOTONIC SHEARING

All monotonic tests were completed under drained shearing conditions using a shearing rate of 0.5 % shear strain per minute. During drained monotonic shearing events, measurements of applied shear stresses, shear strains, and axial strains were recorded. Shearing events were terminated for all tests when specimens achieved single amplitude shear strains (SASS) of 24 %.

UNDRAINED CYCLIC SHEARING

All undrained cyclic tests were completed under equivalent undrained (constant volume) conditions with no actual pore pressure measurements. For all tests, uniform stress-controlled cycles were applied at a cyclic stress ratio ($CSR = \tau/\sigma'_{vo}$) of 0.75 and frequency of 0.05 Hz. The applied CSR of 0.75, although relatively large when compared with CSR values traditionally applied to uncemented sands, was selected following earlier results by Lee et al. (2022) in order to ensure that specimens achieved liquefaction triggering within numbers of cycles relevant to earthquake-induced loading applications (≈0 to 100 cycles). Shearing events were terminated when specimens experienced 24 % double amplitude shear strain (DASS). Following cyclic shearing events, applied vertical stresses were unloaded (≈0 kPa), specimens were recentered back to the zero position, and specimens were reconsolidated by applying a vertical stress of 100 kPa. During undrained cyclic shearing events, measurements of applied shear stresses, shear strains, and changes in applied vertical total stresses were recorded.

$CaCO_3$ CONTENT MEASUREMENTS

Following DSS testing, select specimens were subsampled to characterize biocementation magnitudes and uniformity along specimen heights (≈22 mm). Depending on the achieved cementation level, specimens were sectioned into either two or three sections to assess cementation uniformity. Soil $CaCO_3$ content by mass measurements were performed on oven-dried soil subsamples following the pressure chamber method outlined in ASTM D4373-14, *Standard Test Method for Rapid Determination of Carbonate Content of Soils*. A minimum of two soil $CaCO_3$ content measurements were performed for each specimen section, with both average section values and the standard deviation of section values reported. Section values were further averaged for entire specimens to describe average soil $CaCO_3$ contents by mass, as described in **Table 1**.

Copyright by ASTM Int'l (all rights reserved) Tue Jul 18 19:37:22 EDT 2023
Downloaded/printed by
University of Washington pursuant to License Agreement. No further reproductions authorized.

Copyright by ASTM Int'l (all rights reserved) Tue Jul 18 19:37:22 GMT 2023
Downloaded/printed by
University of Washington pursuant to License Agreement. No further reproductions authorized.

TABLE 1
Summary of DSS specimen properties

Specimen Type	Shearing Event	Specimen Name	Initial Uncemented Void Ratio, e_0	Final Void Ratio prior to Shearing, e_f	Initial Uncemented, V_s, m/s	ΔV_s Increases from Cementation, m/s	ΔV_s Decreases from Dissolution, m/s	Overall ΔV_s Increases prior to Shearing, m/s	Average $CaCO_3$ Content prior to Shearing, %
Uncemented (U)	Drained monotonic (DM)	Uncem-Mono-Loose	0.72	0.72	150				
Uncemented (U)	Drained monotonic (DM)	Uncem-Mono-Med Dens	0.65	0.65	159				
Nondegraded cemented (C)	Drained monotonic (DM)	Cem-Mono-ΔV_s 136 m/s	0.68	0.67	150	137		137	0.6
Nondegraded cemented (C)	Drained monotonic (DM)	Cem-Mono-ΔV_s 250 m/s	0.67	0.65	160	250		250	1.5
Nondegraded cemented (C)	Drained monotonic (DM)	Cem-Mono-ΔV_s 485 m/s	0.70	0.63	159	485		485	4.5
Nondegraded cemented (C)	Undrained cyclic (UC)	Cem-Cyc-ΔV_s 156 m/s	0.70	0.69	162	156		156	0.7
Nondegraded cemented (C)	Undrained cyclic (UC)	Cem-Cyc-ΔV_s 247 m/s	0.70	0.67	156	247		247	2.1
Degraded cemented (D)	Drained monotonic (DM)	Degrad Cem-Mono-ΔV_s 227 to 120 m/s	0.69	0.67	151	227	107	120	1.1
Degraded cemented (D)	Drained monotonic (DM)	Degrad Cem-Mono-ΔV_s 480 to 283 m/s	0.68	0.63	159	480	197	283	3.3
Degraded cemented (D)	Undrained cyclic (UC)	Degrad Cem-Cyc-ΔV_s 260 to 168 m/s	0.68	0.66	149	260	92	168	1.6

SCANNING ELECTRON MICROSCOPE IMAGING

Scanning electron microscope (SEM) imaging was performed to evaluate potential differences in cementation morphology and microstructure following the chemical degradation of biocemented sands. Subsamples from four different DSS specimens subjected to drained monotonic shearing were used for imaging, including the uncemented loose specimen, the nondegraded biocemented specimen with a ΔV_s of 250 m/s, the degraded biocemented specimen initially cemented to a ΔV_s of 227 m/s and degraded to 120 m/s, and the degraded biocemented specimen cemented to a ΔV_s of 480 m/s and degraded to 283 m/s. SEM imaging was performed using an FEI XL830 dual-beam focused ion beam SEM (FEI Co., Hillsboro, OR). Specimen subsamples were prepared for imaging by oven-drying soil samples for at least 24 h, mounting soil subsamples on the surface of imaging pedestals using carbon tape, and sputter-coating materials using a 60 % gold/40 % palladium alloy to improve image resolution.

Results and Discussion

SPECIMEN PROPERTIES

Table 1 summarizes all DSS specimen properties including the type of specimen (i.e., uncemented, nondegraded biocemented, degraded biocemented), the applied shearing event (i.e., drained monotonic, undrained cyclic), specimen names, initial void ratio (e_0) values, final void ratio (e_f) values prior to shearing (accounting for added $CaCO_3$ masses when present), initial V_s values, ΔV_s increases from cementation, ΔV_s decreases from degradation, overall ΔV_s increases prior to shearing (accounting for both cementation increases and degradation-induced decreases, when applicable), and average soil $CaCO_3$ contents. As shown, all nondegraded and degraded biocemented specimens had initial void ratio values between 0.70 and 0.68 ($D_r \approx 30$ and 42 %), which were similar to the uncemented loose specimen. However, following biocementation, specimen void ratios were reduced through the precipitation of added mineral solids, with final void ratio values in cemented specimens oftentimes being more similar to the medium dense uncemented specimen ($e_0 = 0.65$). As shown, seven drained monotonic tests were performed, which included two uncemented specimens prepared to loose ($e_0 = 0.72$, $D_r \approx 32$ %) and medium dense ($e_0 = 0.65$, $D_r \approx 54$ %) conditions; three nondegraded biocemented specimens that were prepared initially loose and were cemented to achieve ΔV_s values of 137, 250, and 485 m/s; a degraded biocemented specimen that was prepared loose, biocemented to a ΔV_s of 227 m/s, and subsequently chemically degraded to a ΔV_s of 120 m/s; and another degraded biocemented specimen that was prepared loose, biocemented to a ΔV_s of 480 m/s, and subsequently chemically degraded to a ΔV_s of 283 m/s. Similar specimens were also considered for undrained cyclic tests; however, uncemented specimens could not be tested because of the relatively high CSR value of 0.75 that was applied, which resulted in failure of the uncemented specimen monotonically prior to achieving the targeted shear stress (failure in less than 0.25 cycles). Instead, for undrained cyclic tests, two initially nondegraded biocemented specimens were prepared initially loose ($e_0 = 0.70$, $D_r \approx 30$ to 34 %) and were biocemented to ΔV_s values of 156 and 247 m/s, and a single degraded biocemented specimen was prepared initially loose, biocemented to a ΔV_s of 260 m/s, and subsequently degraded to a ΔV_s of 168 m/s. The considered specimens allowed for the effect of biocementation and chemically induced damage to be evaluated at similar ΔV_s values and the effect of cementation-induced void ratio reductions to be controlled for through tests on denser uncemented specimens.

CEMENTATION AND DISSOLUTION PROGRESSION

V_s measurements have been shown to have a near-linear relationship with added soil $CaCO_3$ contents (Gomez and DeJong 2017; Lee et al. 2022) and were therefore performed during treatments applied to DSS specimens in order to nondestructively monitor increases in soil small-strain shear stiffnesses resulting from biocementation and assess chemical damage resulting from degradation injections. Figure 1 presents changes in biocemented specimen shear wave velocities (ΔV_s) versus elapsed time for the five nondegraded biocemented specimens and the three degraded biocemented specimens examined in both the monotonic and cyclic tests. As shown, the five nondegraded biocemented specimens received cementation injections over 1 to 3 days

Copyright by ASTM Int'l (all rights reserved) Tue Jul 18 19:37:22 EDT 2023
Downloaded/printed by
University of Washington pursuant to License Agreement. No further reproductions authorized.

FIG. 1

Changes in DSS specimen shear wave velocities (ΔV_s) versus elapsed time for five nondegraded biocemented specimens and three degraded biocemented specimens examined in both drained monotonic and undrained cyclic DSS tests.

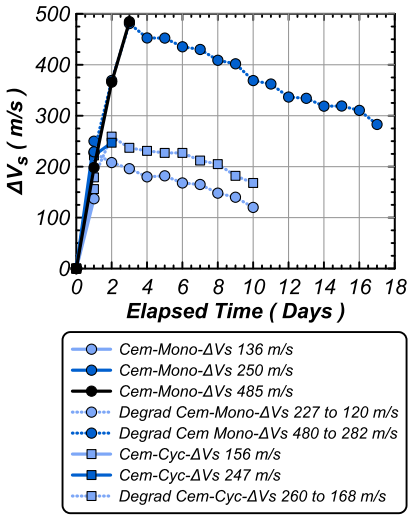

dependent on the targeted cementation level and achieved ΔV_s increases between 136 and 485 m/s. The three degraded biocemented specimens also received cementation injections over a similar time period and achieved ΔV_s increases between 250 and 480 m/s; however, following cementation, 4 to 7 degradation injections were subsequently applied once every 48 h over 8 to 14 days to reduce ΔV_s values by approximately 100 and 200 m/s, respectively. As shown, in both degraded biocemented specimens, ΔV_s values decreased by approximately 25 m/s for every degradation injection. After all treatments were completed, final V_s measurements were obtained for all specimens to characterize the conditions present immediately prior to shearing and shearing events were initiated.

Following mechanical testing, six select DSS specimens representative of the considered cementation levels were destructively subsampled and soil $CaCO_3$ contents by mass were determined as a function of distance from the solution injection location. Soil $CaCO_3$ contents were obtained for specimen samples collected immediately following shearing events and thus reflected the specimen conditions present during shearing. As shown in **figure 2**, all specimens achieved relatively uniform soil $CaCO_3$ contents following both cementation as well as after chemical degradation, when present, with no significant cementation gradients observed along specimen heights. Although three section measurements were obtained for almost all specimens, the nondegraded biocemented specimen prepared to the highest cementation level sample (ΔV_s of 485 m/s) could not be easily sampled into three sections, and therefore only two sections were measured. As shown, nondegraded biocemented specimens achieved average $CaCO_3$ contents between 0.6 and 0.7 % by mass for ΔV_s values between 136 and 156 m/s, average $CaCO_3$ contents between 1.5 and 2.1 % by mass for ΔV_s values between 247 and 250 m/s, and an average $CaCO_3$ content of 4.5 % for a ΔV_s value of 485 m/s. However, when specimens were first cemented to ΔV_s values between 227 and 260 m/s and subsequently chemically degraded to ΔV_s values between 120 and 168 m/s, average $CaCO_3$ contents were between 1.1 and 1.6 % by mass, which were considerably larger than nondegraded biocemented specimens for similar ΔV_s values. Similar trends were also observed at higher cementation levels with the degraded biocemented specimen cemented to a ΔV_s value of 480 m/s and degraded to ΔV_s of 287 m/s having an average $CaCO_3$ content of 3.3 % by mass, which was again significantly larger than the values reported for the nondegraded biocemented specimens prepared to similar ΔV_s values (average $CaCO_3$ contents between 1.5 and 2.1 % by mass). Although the specific mechanisms responsible for this difference remain unclear, it is suspected that degradation injections may have preferentially dissolved biocementation at interparticle contacts, with greater $CaCO_3$ remaining within

Copyright by ASTM Int'l (all rights reserved) Tue Jul 18 19:37:22 EDT 2023
Downloaded/printed by
University of Washington pursuant to License Agreement. No further reproductions authorized.

FIG. 2 Soil $CaCO_3$ content by mass distributions for three nondegraded biocemented specimens and three degraded biocemented specimens representative of the different cementation levels considered in this study ($\Delta V_s \approx 150$ to 500 m/s). Provided distributions represent conditions present immediately prior to shearing events for all samples. Error bars indicate one standard deviation for each section's $CaCO_3$ content measurements.

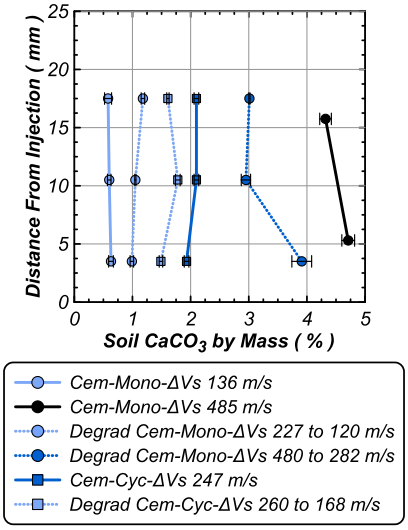

degraded samples on soil particle surfaces and within free pore space, both of which would be expected to have more minimal effects on small-strain stiffness enhancements.

DRAINED MONOTONIC SHEARING

Figure 3 presents results from drained monotonic tests performed on uncemented, nondegraded biocemented, and degraded biocemented specimens including shear stress versus shear strain (fig. 3*A*) and axial strain versus shear strain (fig. 3*B*) responses. As shown, large differences in specimen drained shearing behaviors were observed as a function of both cementation level and initial void ratios (for uncemented tests). As expected, uncemented specimens prepared to loose ($e_0 = 0.72$, $D_r \approx 32$ %) and medium dense ($e_0 = 0.65$, $D_r \approx 54$ %) conditions were initially contractive and exhibited strain hardening responses with much lower initial shear stiffnesses and shear strengths when compared with biocemented specimens at similar strain levels. The modest effect of small decreases in specimen void ratios on uncemented specimen behaviors suggested that the observed responses in the biocemented specimens could be primarily attributed to the presence of biocementation bonding and could not be fully explained by the associated reductions in specimen void ratios resulting from added mineral solids. In the nondegraded biocemented specimens prepared to ΔV_s values of 136, 250, and 485 m/s, significantly higher peak strengths and shear stiffnesses were observed with increasing cementation. For example, although the uncemented loose specimen achieved a peak shear strength near ≈50 kPa, the peak shear strength for the ΔV_s of 250 m/s specimen was near ≈66 kPa, and the peak shear strength for the most heavily cemented specimen ($\Delta V_s =$ 485 m/s) was nearly 3 times larger than the uncemented value (near ≈150 kPa). When compared with the uncemented specimens, peak strengths for cemented specimens were also observed at significantly smaller strain levels (SASS near 0.5 %) with minimal volumetric strains observed at peak strength. As cementation levels increased above ΔV_s values near 250 m/s, a notable transition from strain hardening to strain softening behavior was also observed. At larger strains postpeak, however, cemented bonds were increasingly damaged and could no longer restrict volumetric changes, with strong dilation observed because of the presence of added mineral solids and increases in particle angularity from cemented particle coatings. The most highly cemented specimens

Copyright by ASTM Int'l (all rights reserved) Tue Jul 18 19:37:22 EDT 2023
Downloaded/printed by
University of Washington pursuant to License Agreement. No further reproductions authorized.

FIG. 3

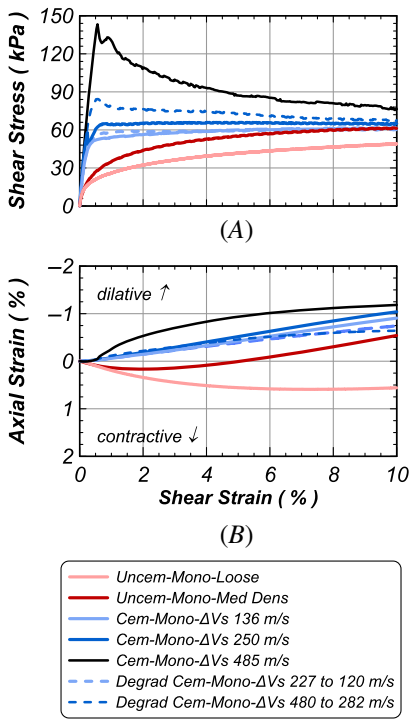

Results from drained monotonic tests including (*A*) shear stress and (*B*) axial strain versus shear strain responses for tests performed on uncemented specimens at 2 different initial densities, 3 nondegraded biocemented specimens prepared to ΔV_s values of 136, 250, and 485 m/s, and 2 degraded biocemented specimens initially cemented to higher cementation levels but degraded to final ΔV_s values of 120 and 282 m/s.

($\Delta V_s = 250$ and 485 m/s) maintained detectably higher shear strengths at large strains, likely because of these particle level changes, whereas all other less cemented and uncemented specimens appeared to converge at large strains despite not yet reaching constant volume conditions.

When examining the response of the degraded biocemented specimen, which had a final ΔV_s value of 120 m/s, interestingly, the shearing behavior was similar to the nondegraded biocemented specimen with a ΔV_s of 136 m/s. The degraded biocemented specimen had both a lower ΔV_s (16 m/s less) and a higher average $CaCO_3$ content (0.5 % greater) when compared with the nondegraded specimen yet exhibited a slightly higher peak strength and was also slightly less dilative at larger strains. When examining behaviors at higher cementation levels, the degraded biocemented specimen with a final ΔV_s value of 283 m/s exhibited a higher peak strength (≈84 kPa) when compared with the nondegraded biocemented specimen (≈66 kPa), which had a similar ΔV_s of 250 m/s but a considerably lower average calcite content (1.8 % by mass lower). Interestingly, the degraded specimen exhibited less dilatation at similar strains despite having a higher peak strength, potentially indicating greater retention of cementation bonding at higher strain than the nondegraded specimen, which could restrict dilation. This is also somewhat reflected in the slightly elevated shear strengths observed at larger strains in the degraded specimen when compared with the nondegraded specimen. These behavioral differences were somewhat counterintuitive because similar ΔV_s values, which largely reflect the integrity of the cemented bonds, would be expected to result in more similar peak strengths, and higher soil $CaCO_3$ contents, which largely reflect specimen dry density differences, would be expected to result in stronger dilatancy at larger strains. Although such results suggest that significant differences in specimen microstructures may occur following chemical damage, collectively, these responses suggest from a pragmatic perspective that the drained shearing behavior of degraded biocemented specimens may be at least comparable with responses observed for nondegraded biocemented specimens at similar ΔV_s values. Further investigations, however, may shed further light on the role of chemical

Copyright by ASTM Int'l (all rights reserved) Tue Jul 18 19:37:22 EDT 2023
Downloaded/printed by
University of Washington pursuant to License Agreement. No further reproductions authorized.

damage in influencing the relationships between peak shear strengths and ΔV_s values as well as volumetric tendencies observed during shearing.

UNDRAINED CYCLIC SHEARING

Undrained cyclic DSS tests were performed for two nondegraded biocemented specimens prepared to ΔV_s values of 156 and 247 m/s as well as a single degraded biocemented sample that was initially cemented to a ΔV_s value of 260 m/s and then subsequently degraded to a ΔV_s value of 168 m/s. All tests were prepared initially loose, subjected to a CSR of 0.75, and sheared until a DASS of 24 % was achieved. Following shearing, specimens were reconsolidated, and postshearing V_s measurements were performed. **Table 2** presents a summary of all undrained cyclic DSS test results including specimen type, specimen name, overall ΔV_s increases prior to shearing (accounting for both cementation increases and dissolution decreases, when applicable), average soil $CaCO_3$ contents, the applied CSR, and various metrics describing liquefaction triggering behaviors (i.e., cycles to SASS = 3 %, cycles to $r_u = 0.95$) and post-triggering behaviors (i.e., cycles to SASS = 9 %, cycles to DASS = 24 %, reconsolidation strains, and ΔV_s decreases following shearing and reconsolidation).

Figure 4 presents results from undrained cyclic tests on the two nondegraded biocemented specimens and the single degraded biocemented specimen. As shown, large differences in liquefaction triggering resistances and post-triggering behaviors were observed with differences in cementation level and chemical damage. For example, the ΔV_s of 156 m/s nondegraded biocemented specimen achieved triggering (3 % SASS) after approximately 0.7 cycles, whereas the more heavily biocemented ΔV_s of 247 m/s specimen required 29.2 cycles to achieve triggering. When comparing the response of the degraded biocemented specimen, which had a ΔV_s value of 167 m/s, triggering was achieved after 1.6 cycles, a small improvement over the nondegraded biocemented specimen that had a slightly smaller ΔV_s. Following liquefaction triggering, benefits at larger strains were also observed with increasing cementation. For example, when examining post-triggering strain accumulation, the number of cycles to 24 % DASS increased from 2.1 to 40.2 cycles as ΔV_s values increased from 156 to 247 m/s for the nondegraded biocemented specimens. Following chemical degradation, however, the degraded biocemented specimen ($\Delta V_s =$ 168 m/s) exhibited post-triggering strain accumulation behavior that was again consistent with the nondegraded biocemented specimen at a similar ΔV_s (156 m/s) with a slightly larger 5.4 cycles required to achieve 24 % DASS. When examining reconsolidation behaviors, only small reductions in reconsolidation strains were observed as a function of cementation level with the chemically degraded specimen having the lowest reconsolidation strain of all specimens (1.5 %). However, all biocemented specimens achieved strains between 1.5 and 1.8 %, which were similar to strains near the 2 % values observed for loose uncemented specimens sheared to 24 % DASS and reconsolidated using similar testing procedures (Lee et al. 2022). Although uncemented tests were not performed because of the large applied CSR of 0.75, which would have triggered liquefaction in uncemented specimens prior to achieving the target shear stress of 75 kPa (i.e., triggering in less than 0.25 cycles), significant dilation was observed initially during undrained cyclic shearing for all biocemented specimens, with r_u values near −0.4 observed at the start of loading and progressive increases in positive r_u generation with added cycles during stress reversals as cemented bonds became increasingly damaged and specimens became increasingly contractive. Finally, following shearing events and reconsolidation, V_s measurements suggested that ΔV_s increases following biocementation were largely erased following shearing and reconsolidation for both the nondegraded and degraded biocemented specimens, reflective of significant damage to cemented microstructures following shearing to 24 % DASS. Similar to previous drained monotonic shearing behaviors, results from undrained cyclic tests suggest that the shearing behavior of chemically degraded biocemented specimens appears to be consistent with nondegraded biocemented specimens when evaluated on the basis of ΔV_s values. Interestingly, however, these behaviors do not agree on the basis of soil $CaCO_3$ contents, which were consistently higher in the degraded specimens at similar ΔV_s values. This discrepancy may result from the ability of V_s measurements to more effectively capture the integrity of cemented bonds, whereas soil $CaCO_3$ contents solely describe the total mass of cementing minerals but do not provide insights regarding the interparticle distributions of cementation (i.e., at

Copyright by ASTM Int'l (all rights reserved) Tue Jul 18 19:37:22 EDT 2023
Downloaded/printed by
University of Washington pursuant to License Agreement. No further reproductions authorized.

TABLE 2

Summary of results from undrained cyclic tests

Specimen Properties				Loading	Triggering		Post-Triggering			
Specimen Type	Specimen Name	Overall ΔV_s Increases prior to Shearing, m/s	Average $CaCO_3$ Content, %	CSR	Cycles to 3 % SASS	Cycles to $r_u = 0.95$	Cycles to 9 % SASS	Cycles to 24 % DASS	Reconsolidation Strain, %	ΔV_s Decreases after Shearing and Reconsolidation, m/s
Nondegraded cemented (C)	Cem-Cyc-ΔV_s 156 m/s	+156	0.7	0.75	0.7	1.5	1.6	2.1	1.8	−166
Nondegraded cemented (C)	Cem-Cyc-ΔV_s 247 m/s	+247	2.1	0.75	29.2	26.5	38.2	40.2	1.7	−244
Degraded cemented (D)	Degrad Cem-Cyc-ΔV_s 260 to 168 m/s	+168	1.6	0.75	1.6	3.0	3.5	5.4	1.5	−163

Copyright by ASTM Int'l (all rights reserved) Tue Jul 18 19:37:22 GMT 2023
Downloaded/printed by
University of Washington pursuant to License Agreement. No further reproductions authorized.

FIG. 4 Results from undrained cyclic tests on biocemented specimens prepared to ΔV_s values of (*A*) 156 m/s and (*B*) 247 m/s as well as (*C*) degraded biocemented specimens that were prepared to a ΔV_s value of 260 m/s and then degraded to a ΔV_s value of 168 m/s. Plots present (*i*) shear stress versus vertical effective stress, (*ii*) shear stress versus shear strain, and (*iii*) excess pore pressure ratio ($r_u = \Delta u/\sigma_v'$) versus cycle number. All specimens were prepared initially loose ($D_r \approx 35$ %) and were subjected to a CSR of 0.75.

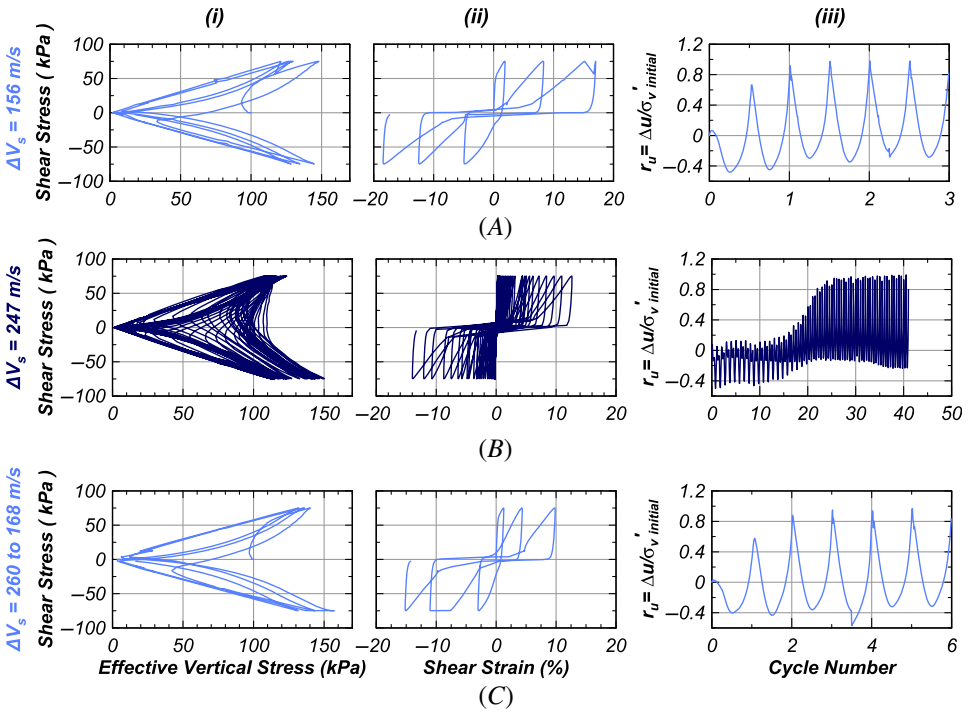

particle contacts versus within open pore space versus on particle surfaces), which may be key to understanding the afforded mechanical responses.

EFFECT OF DISSOLUTION ON CEMENTED MICROSTRUCTURES

Figure 5 presents representative SEM images of select uncemented, nondegraded biocemented, and degraded biocemented sand DSS specimens subjected to drained monotonic shearing. Subsamples that were imaged were obtained from the loose uncemented specimen (fig. 5*A*–*C*), the nondegraded biocemented specimen with a ΔV_s of 250 m/s (fig. 5*D*–*F*), the degraded biocemented specimen that was cemented to a ΔV_s of 227 m/s and was then degraded to a ΔV_s of 120 m/s (fig. 5*G*–*I*), and the degraded biocemented specimen that was cemented to a ΔV_s of 480 m/s and was then degraded to a ΔV_s of 283 m/s (fig. 5*J*–*L*). As shown, clean quartz surfaces are observed in the uncemented specimen with no evidence of mineral precipitation (fig. 5*C*). In the nondegraded specimen, however, well-formed rhombohedral crystals are observed across particle surfaces, which are consistent with morphologies expected for calcite (fig. 5*F*). Once specimens were degraded, however, new crystal morphologies were observed that look increasingly weathered, with some crystals appearing to be fragmented with the internal structure visible (fig. 5*I*–*L*). Furthermore, the crystals remaining after degradation appear to be somewhat more weakly associated with particle surfaces with more frequent loose crystals observed in images (fig. 5*I*–*L*). Although it should be mentioned that the imaged subsamples were destructively sampled and obtained after shearing events, the observed differences in cemented microstructures following chemical degradation suggested that although significant $CaCO_3$ remained within the chemically damaged biocemented specimens, the applied

Copyright by ASTM Int'l (all rights reserved) Tue Jul 18 19:37:22 EDT 2023
Downloaded/printed by
University of Washington pursuant to License Agreement. No further reproductions authorized.

FIG. 5 SEM images of subsamples from select DSS specimens subjected to drained monotonic shearing. Presented images are from (*A–C*) the uncemented loose specimen, (*D–F*) the nondegraded biocemented specimen with a ΔV_s of 250 m/s, (*G–I*) the degraded biocemented specimen with a final ΔV_s of 120 m/s, and (*J–L*) the degraded biocemented specimen with a final ΔV_s of 283 m/s. Images were obtained at magnifications of (*A*, *D*, *G*, *J*) ×100, (*B*, *E*, *H*, *K*) ×200, and (*C*, *F*, *I*, *L*) ×1,000.

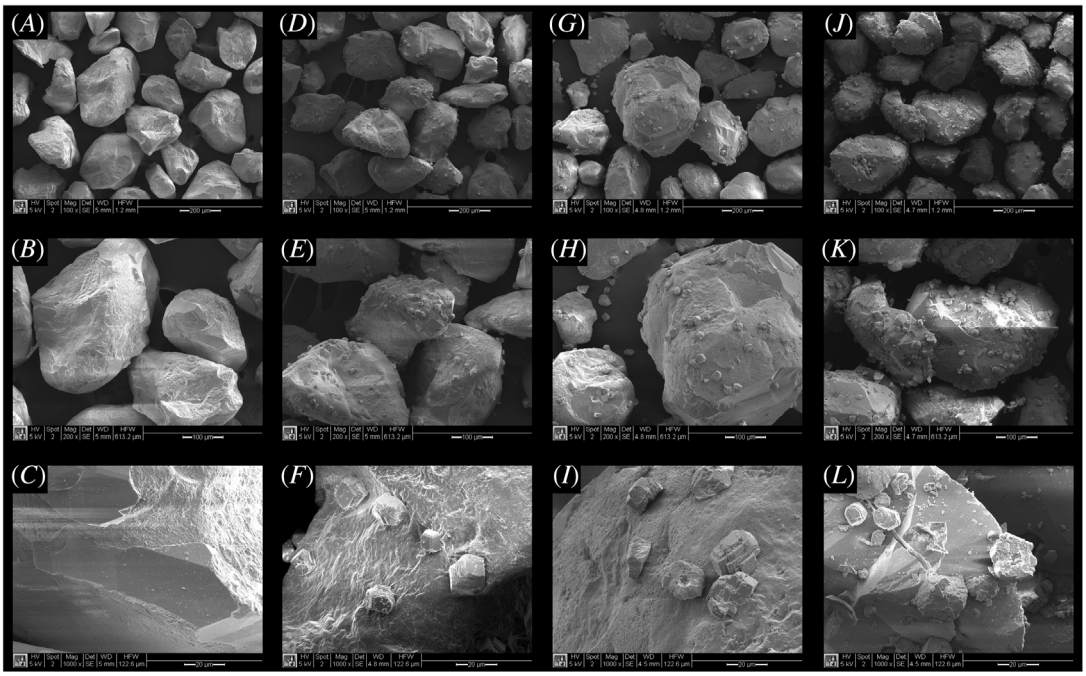

degradation injections may have altered $CaCO_3$ crystal integrities and could have resulted in the cementation becoming more weakly associated with soil particle surfaces. This observation may help explain why degraded biocemented specimens maintained relatively high soil $CaCO_3$ contents when compared with nondegraded biocemented specimens at similar ΔV_s values. Despite these large changes in cemented microstructures, however, V_s measurements were still shown to effectively discern mechanical improvements afforded by biocementation, independent of whether chemically induced damage was present or not.

Conclusions

A study was performed to investigate the effect of chemically induced damage on the shearing behavior of biocemented sands. Seven DSS tests were performed to examine the drained monotonic shearing behavior of two uncemented sand specimens prepared to different relative densities, nondegraded biocemented loose sand specimens prepared to three different ΔV_s magnitudes between 150 and 485 m/s, and two chemically degraded biocemented specimens that were cemented to higher cementation levels and then degraded to final ΔV_s values of either 120 or 283 m/s. Three additional DSS tests were then performed to further examine the undrained cyclic shearing behaviors of both nondegraded and degraded biocemented sand specimens prepared to similar cementation levels as those considered in earlier monotonic tests. Following all tests, specimen cementation levels were characterized, and the effect of cementation magnitudes and chemically induced damage on drained monotonic shearing behaviors, including volumetric changes and peak strengths, and undrained cyclic shearing behaviors, including liquefaction triggering and post-triggering consequences, were explored. From the results of this study, the following conclusions can be made:

Copyright by ASTM Int'l (all rights reserved) Tue Jul 18 19:37:22 EDT 2023
Downloaded/printed by
University of Washington pursuant to License Agreement. No further reproductions authorized.

- A novel microbial fermentation cementation degradation process was employed and allowed for the preparation of degraded biocemented specimens with uniform material properties. The developed techniques allowed for the preparation of specimens with homogeneous chemical damage that were expected to be representative of the response of degraded biocemented soils, which may be present at various field sites following initial biocementation applications.
- Following chemical degradation, degraded biocemented sand specimens had larger soil $CaCO_3$ contents than nondegraded biocemented sand specimens at similar ΔV_s values. Differences in cementation morphologies were also visually observed following chemical degradation, with noticeable surficial deterioration and an apparent weaker association of precipitates with soil particle surfaces.
- When examining differences in drained monotonic shearing behaviors, nondegraded biocemented specimens exhibited large increases in initial shear stiffness and peak shear strength with increasing cementation levels. Similar to observations from other past studies, biocemented specimens exhibited minimal volumetric changes at peak strength, with dilatancy increasingly mobilized postpeak, following the degradation of cemented bonds because of increases in particle angularity and surface roughness as well as the addition of added mineral solids. Following chemical degradation, shearing behaviors for the degraded biocemented specimens were largely consistent with nondegraded biocemented specimens when comparing responses at similar ΔV_s values.
- When examining undrained cyclic shearing responses, liquefaction triggering and post-triggering behaviors were again consistent between nondegraded and degraded biocemented specimens on the basis of ΔV_s.
- V_s measurements were shown to effectively track changes in biocemented soil mechanical behaviors independent of the presence of chemical damage. Although soil $CaCO_3$ contents are routinely reported for laboratory tests involving biocemented soils, the results of this study suggest that such measurements may provide only limited insights regarding expected engineering behaviors, particularly when chemical damage is present. Moving forward, V_s measurements may offer a superior metric for the assessment of long-term cementation integrity following field applications and an improved ability to compare laboratory and field responses.
- Although the performed tests provide the first characterization of the mechanical behavior of biocemented soils following chemical damage, further work remains needed to more fully understand these engineering behaviors. Such insights will likely be critical for improving our understanding of the life-cycle performance of biocementation soil improvement and identifying metrics by which cementation integrity can be effectively evaluated following field applications.

ACKNOWLEDGMENTS

Funding for this research work was provided by the National Science Foundation (ECI-1824647) and is greatly appreciated. Collaboration made possible through the Engineering Research Center Program of the National Science Foundation under NSF Cooperative Agreement No. EEC-1449501 is also acknowledged. Any opinions, findings, and conclusions or recommendations expressed in this manuscript are those of the authors and do not necessarily reflect the views of the National Science Foundation. Presented SEM images were made possible by the Molecular Analysis Facility, a National Nanotechnology Coordinated Infrastructure site at the University of Washington that is supported in part by the National Science Foundation Grant NNCI-1542101, the University of Washington, the Molecular Engineering and Sciences Institute, and the Clean Energy Institute. Research assistance from Scott Braswell and Samantha Young is appreciated.

References

ASTM International. 2017. *Standard Practice for Classification of Soils for Engineering Purposes (Unified Soil Classification System)*. ASTM D2487-17. West Conshohocken, PA: ASTM International, approved April 2, 2020. https://doi.org/10.1520/D2487-17

ASTM International. 2014. *Standard Test Method for Rapid Determination of Carbonate Content of Soils*. ASTM D4373-14. West Conshohocken, PA: ASTM International, approved June 25, 2021. https://doi.org/10.1520/D4373-14

Copyright by ASTM Int'l (all rights reserved) Tue Jul 18 19:37:22 EDT 2023
Downloaded/printed by
University of Washington pursuant to License Agreement. No further reproductions authorized.

Burdalski, R. J., B. G. O. Ribeiro, M. G. Gomez, and D. Gorman-Lewis. 2022. "Mineralogy, Morphology, and Reaction Kinetics of Ureolytic Bio-cementation in the Presence of Seawater Ions and Varying Soil Materials." *Scientific Reports* 12, no. 1 (October): 17100. https://doi.org/10.1038/s41598-022-21268-3

Cardoso, R., J. Vieira, and I. Borges. 2023. "On the Use of Biocementation to Treat Collapsible Soils." *Engineering Geology* 313 (February): 106971. https://doi.org/10.1016/j.enggeo.2022.106971

Carey, T. J., N. Stone, and B. L. Kutter. 2020. "Grain Size Analysis and Maximum and Minimum Dry Density Testing of Ottawa F-65 Sand for LEAP-UCD-2017." In *Model Tests and Numerical Simulations of Liquefaction and Lateral Spreading*, edited by B. L. Kutter, M. T. Manzari, and M. Zeghal, 31–44. Cham, Switzerland: Springer. https://doi.org/10.1007/978-3-030-22818-7_2

Chen, X. and V. Achal. 2020. "Effect of Simulated Acid Rain on the Stability of Calcium Carbonate Immobilized by Microbial Carbonate Precipitation." *Journal of Environmental Management* 264 (June): 110419. https://doi.org/10.1016/j.jenvman.2020.110419

Cheng, L., M. A. Shahin, and D. Mujah. 2017. "Influence of Key Environmental Conditions on Microbially Induced Cementation for Soil Stabilization." *Journal of Geotechnical and Geoenvironmental Engineering* 143, no. 1 (January): 04016083. https://doi.org/10.1061/(ASCE)GT.1943-5606.0001586

Darby, K. M., G. L. Hernandez, J. T. DeJong, R. W. Boulanger, M. G. Gomez, and D. W. Wilson. 2019. "Centrifuge Model Testing of Liquefaction Mitigation via Microbially Induced Calcite Precipitation." *Journal of Geotechnical and Geoenvironmental Engineering* 145, no. 10: 04019084. https://doi.org/10.1061/(ASCE)GT.1943-5606.0002122

DeJong, J. T., M. G. Gomez, A. C. San Pablo, C. M. R. Graddy, D. C. Nelson, M. Lee, K. Ziotopoulou, B. Montoya, and T. H. Kwon. 2022. "State of the Art: MICP Soil Improvement and Its Application to Liquefaction Hazard Mitigation." In *Proceedings of the 20th ICSMGE-State of the Art and Invited Lectures*, edited by M. Rahman and M. Jaksa, 405–508. London, UK: International Society for Soil Mechanics and Geotechnical Engineering.

Ghasemi, P. and B. M. Montoya. 2022. "Field Implementation of Microbially Induced Calcium Carbonate Precipitation for Surface Erosion Reduction of a Coastal Plain Sandy Slope." *Journal of Geotechnical and Geoenvironmental Engineering* 148, no. 9 (September): 04022071. https://doi.org/10.1061/(ASCE)GT.1943-5606.0002836

Gomez, M. G. and J. T. DeJong. 2017. "Engineering Properties of Bio-cementation Improved Sandy Soils." In *Grouting 2017*, 23–33. Reston, VA: American Society of Civil Engineers. https://doi.org/10.1061/9780784480793.003

Gomez, M. G., B. C. Martinez, J. T. DeJong, C. E. Hunt, L. A. deVlaming, D. W. Major, and S. M. Dworatzek. 2015. "Field-Scale Biocementation Tests to Improve Sands." *Ground Improvement* 168, no. 3 (August): 206–216. https://doi.org/10.1680/grim.13.00052

Gomez, M. G., C. M. Anderson, C. M. R. Graddy, J. T. DeJong, D. C. Nelson, and T. R. Ginn. 2017. "Large-Scale Comparison of Bioaugmentation and Biostimulation Approaches for Biocementation of Sands." *Journal of Geotechnical and Geoenvironmental Engineering* 143, no. 5 (May): 04016124. https://doi.org/10.1061/(ASCE)GT.1943-5606.0001640

Gomez, M. G., C. M. R. Graddy, J. T. DeJong, D. C. Nelson, and M. Tsesarsky. 2018. "Stimulation of Native Microorganisms for Biocementation in Samples Recovered from Field-Scale Treatment Depths." *Journal of Geotechnical and Geoenvironmental Engineering* 144, no. 1 (January): 04017098. https://doi.org/10.1061/(ASCE)GT.1943-5606.0001804

Humire, F., M. Lee, K. Ziotopoulou, M. G. Gomez, and J. T. DeJong. 2022. "Development and Evaluation of Preconditioning Protocols for Sand Specimens in Constant-Volume Cyclic Direct Simple Shear Tests." *Geotechnical Testing Journal* 45, no. 3 (May/June): 661–673. https://doi.org/10.1520/GTJ20210028

Jiang, N.-J. and K. Soga. 2019. "Erosional Behavior of Gravel-Sand Mixtures Stabilized by Microbially Induced Calcite Precipitation (MICP)." *Soils and Foundations* 59, no. 3 (June): 699–709. https://doi.org/10.1016/j.sandf.2019.02.003

Lee, M., M. G. Gomez, M. El Kortbawi, and K. Ziotopoulou. 2022. "Effect of Light Biocementation on the Liquefaction Triggering and Post-triggering Behavior of Loose Sands." *Journal of Geotechnical and Geoenvironmental Engineering* 148, no. 1 (January): 04021170. https://doi.org/10.1061/(ASCE)GT.1943-5606.0002707

Lings, M. L. and P. D. Greening. 2001. "A Novel Bender/Extender Element for Soil Testing." *Géotechnique* 51, no. 8 (September): 713–717. https://doi.org/10.1680/geot.2001.51.8.713

Martinez, B. C. and J. T. DeJong. 2009. "Bio-mediated Soil Improvement: Load Transfer Mechanisms at the Micro-and Macro-scales." In *Advances in Ground Improvement: Research to Practice in the United States and China*, 242–251. Reston, VA: American Society of Civil Engineers. https://doi.org/10.1061/41025(338)26

Montoya, B. M. and J. T. DeJong. 2015. "Stress-Strain Behavior of Sands Cemented by Microbially Induced Calcite Precipitation." *Journal of Geotechnical and Geoenvironmental Engineering* 141, no. 6 (June): 04015019. https://doi.org/10.1061/(ASCE)GT.1943-5606.0001302

Muchongwe, S. T. "Controlling Colloidal Silica Grouts Using Microbial Fermentation Activity." Master's thesis, University of Washington, 2021.

van Paassen, L. A., R. Ghose, T. J. van der Linden, W. R. van der Star, and M. C. van Loosdrecht. 2010. "Quantifying Biomediated Ground Improvement by Ureolysis: Large-scale Biogrout Experiment." *Journal of Geotechnical and Geoenvironmental Engineering* 136, no. 12 (December): 1721–1728. https://doi.org/10.1061/(ASCE)GT.1943-5606.0000382

Ribeiro, B. G. O. and M. G. Gomez. 2023. "Dissolution Behavior of Ureolytic Bio-cementation: Physical Experiments and Reactive Transport Modeling." *Journal of Geotechnical and Geoenvironmental Engineering* 149, no. 9 (September): 04023071. https://doi.org/10.1061/JGGEFK/GTENG-11275

San Pablo, A. C. M., M. Lee, C. M. R. Graddy, C. M. Kolbus, M. Khan, A. Zamani, and N. Martin, et al. 2020. "Meter-Scale Biocementation Experiments to Advance Process Control and Reduce Impacts: Examining Spatial Control, Ammonium

Copyright by ASTM Int'l (all rights reserved) Tue Jul 18 19:37:22 EDT 2023
Downloaded/printed by
University of Washington pursuant to License Agreement. No further reproductions authorized.

By-Product Removal, and Chemical Reductions." *Journal of Geotechnical and Geoenvironmental Engineering* 146, no. 11 (November): 04020125. https://doi.org/10.1061/(ASCE)GT.1943-5606.0002377

Terzis, D., L. Laloui, S. Dornberger, and R. Harran. 2020. "A Full-Scale Application of Slope Stabilization via Calcite Biomineralization Followed by Long-Term GIS Surveillance." In *Geo-Congress 2020*, 65–73. Reston, VA: American Society of Civil Engineers. https://doi.org/10.1061/9780784482834.008

Xiao, P., H. Liu, A. W. Stuedlein, T. M. Evans, and Y. Xiao. 2019. "Effect of Relative Density and Biocementation on Cyclic Response of Calcareous Sand." *Canadian Geotechnical Journal* 56, no. 12 (December): 1849–1862. https://doi.org/10.1139/cgj-2018-0573

Zamani, A., P. Xiao, T. Baumer, T. J. Carey, B. Sawyer, J. T. DeJong, and R. W. Boulanger. 2021. "Mitigation of Liquefaction Triggering and Foundation Settlement by MICP Treatment." *Journal of Geotechnical and Geoenvironmental Engineering* 147, no. 10: 04021099. https://doi.org/10.1061/(ASCE)GT.1943-5606.0002596

Ziotopoulou, K., J. Montgomery, A. M. P. Bastidas, and B. Morales. 2018. "Cyclic Strength of Ottawa F-65 Sand: Laboratory Testing and Constitutive Model Calibration." In *Geotechnical Earthquake Engineering and Soil Dynamics V: Slope Stability and Landslides, Laboratory Testing, and In Situ Testing*, 180–189. Reston, VA: American Society of Civil Engineers. https://doi.org/10.1061/9780784481486.019

Copyright by ASTM Int'l (all rights reserved) Tue Jul 18 19:37:22 EDT 2023
Downloaded/printed by
University of Washington pursuant to License Agreement. No further reproductions authorized.